ACS APPLIED MATERIALS & INTERFACES

Research Article

www.acsami.org

Self-Assembly of Fluorescent Hybrid Core–Shell Nanoparticles and Their Application

Chun Wang, Fu Tang,* Xiaoyu Wang, and Lidong Li*

School of Materials Science and Engineering, University of Science and Technology Beijing, Beijing 100083, P. R. China

ABSTRACT: In this work, a fluorescent hybrid core–shell nanoparticle was prepared by coating a functional polymer shell onto silver nanoparticles via a facile one-pot method. The biomolecule poly-L-lysine (PLL) was chosen as the polymer shell and assembled onto the silver core via the amine-reactive cross-linker, 3,3′-dithiobis(sulfosuccinimidylpropionate). The fluorescent anticancer drug, doxorubicin, was incorporated into the PLL shell through the same linkage. As the cross-linker possesses a thiol-cleavable disulfide bond, disassembly of the PLL shell was observed in the presence of glutathione, leading to controllable doxorubicin release. The silver core there provided an easily modified surface to facilitate the shell coating and ensures the efficient separation of as-prepared nanoparticles from their reaction mixture through centrifugation. Cell assays show that the prepared hybrid fluorescent nanoparticles can internalize into cells possessing excellent biocompatibility prior to the release of doxorubicin, terminating cancer cells efficiently as the doxorubicin is released at the intracellular glutathione level. Such properties are important for designing smart containers for target drug delivery and cellular imaging.

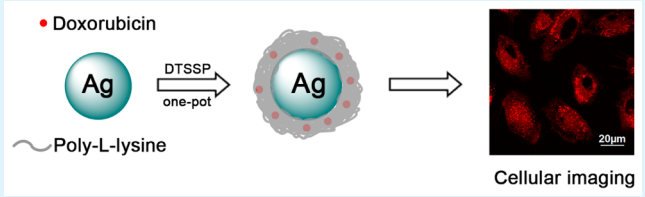

KEYWORDS: *fluorescence, polymer, core–shell nanoparticles, self-assembly, disassembly, cellular imaging*

INTRODUCTION

Research on nanostructured materials over recent decades has gained much attention because of the ability to tailor the chemical and physical properties by simply varying their size, composition, and structural order. Therefore, considerable effort has been devoted to the design and fabrication of nanocomposites with desired functionalities.[1−9] Among them, hybrid nanocomposites with core–shell structures have attracted much interest for their unique advantages that can combine diverse functionalities of materials (the core and the shell) into one entity. Moreover, such core–shell materials usually exhibit features that are different to the individual entities, and in some cases the synergy is superior to their single-component counterparts.[10−12] To fabricate a core–shell structured nanoparticle, one typical procedure involves encapsulating a colloidal core (i.e., organic, inorganic, or metal nanoparticle) with a special shell, so as to modify the surface properties of the core component.[13−22]

An abundance of materials can be adopted to fabricate the shell. Polymer shells possess advantages for their synthetic versatility and the flexibility of the polymer chain. In regard to polymer-shell-coated nanoparticles, there has been a wealth of research in relation to functionalization of the polymers in addition to the permeability of the polymer shells.[23−26] Polymer-shell permeability typically depends on the nature of the polymers, especially when stimuli-responsive polymers are used. For example, by fabricating the polymer shell with weak and strong polyelectrolytes via "layer-by-layer" self-assembly, the permeability of the polymer shell can be tuned by changes in environmental factors such as pH and ionic strength.[27−30] Furthermore, synthesis of thermoresponsive polymers cross-linked onto nanoparticles result in tailoring of the permeability of the as-prepared polymer shell as a function of temperature. Thus, controllable permeability of polymer shells can be achieved by employing various stimuli-responsive polymers.[31−34]

Meanwhile, the stimuli are not restricted to the above-mentioned common triggers. Additional stimuli can be extended to biomacromolecules and small molecules (e.g., glucose, enzymes, and glutathione (GSH)) that are inherently present in biological systems.[35−38] Polymer particles and capsules constructed by these functional polymers have been intentionally designed as specific biosensors and smart delivery vehicles for controlled drug storage/release applications.[39−43] However, such materials are only formed via time-consuming synthesis and separation processes.

In this work, we reported a facile one-pot method to fabricate a fluorescent core–shell structured nanoparticle composed of a silver (Ag) nanoparticle core and a biocompatible polymer shell—the biomolecule poly-L-lysine, (PLL). The PLL molecules were cross-linked and assembled onto silver nanoparticle surfaces by a primary amine-reactive cross-linker 3,3′-dithiobis(sulfosuccinimidylpropionate) (DTSSP). At the same time, the commonly used fluorescent anticancer drug, doxorubicin (DOX), was incorporated into the PLL shell via the same linkage. As DTSSP contains a thiol-reducible disulfide bond, when stimulated in the presence of GSH, the disulfide bond is cleaved. This leads to a gradual disassembly of the PLL

Received: April 21, 2015
Accepted: June 2, 2015
Published: June 2, 2015

DOI: 10.1021/acsami.5b03440
ACS Appl. Mater. Interfaces 2015, 7, 13653−13658

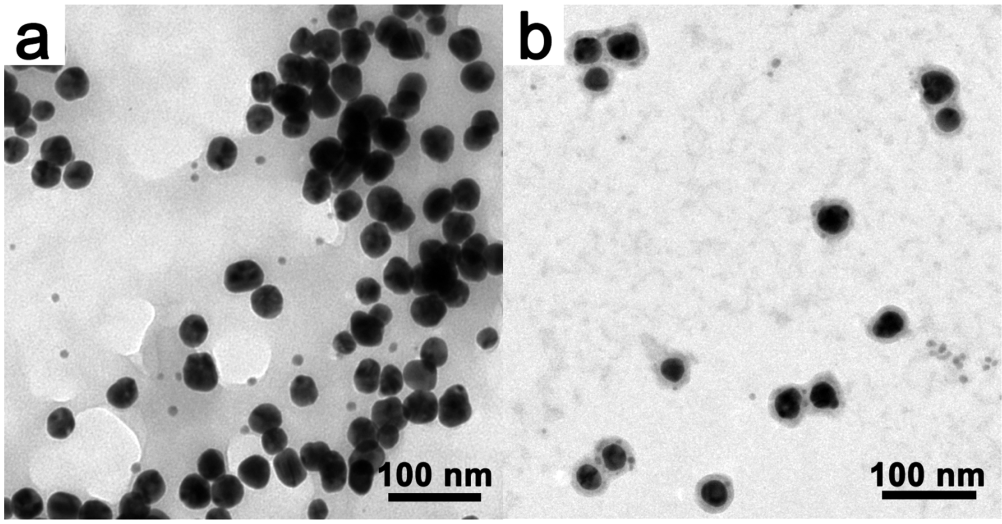

Figure 1. TEM micrographs of (a) Ag and (b) Ag@PLL-DOX nanoparticles.

molecules and the release of DOX, allowing this controllable release process upon GSH stimuli to be detected via monitoring the fluorescence change of DOX.

The silver core was premodified with amino groups to facilitate the PLL shell coating, and the heavier mass of the silver core increases the separation efficiency of the prepared nanoparticles from their reaction mixture via centrifugation. The size of the prepared core−shell nanoparticles are suitably tailored to ensure rapid internalization into cells, as evidenced by cellular imaging assaying. Furthermore, both the release and cell viability assays show that the as-prepared nanoparticles possess good biocompatibility before the release of DOX at low GSH concentrations, and at increased concentrations terminate cancer cells efficiently. Such properties are important for designing smart containers for specific drug-delivery applications and cellular imaging.

EXPERIMENTAL SECTION

Materials and Measurements. Cystamine dihydrochloride and GSH were purchased from J&K Chemical Co. Silver nitrate, DOX, and DTSSP were purchased from Sigma-Aldrich. PLL (M_w = 30 000−70 000) was purchased from Beijing Biodee Biotechnology Co. Other reagents used in the experiments were purchased from J&K Chemical or Sigma-Aldrich, and were used without further purification, unless otherwise stated. Distilled water was used. Ultraviolet−visible (UV−vis) absorption spectra were collected on a Hitachi U-3900H spectrophotometer. Fluorescence spectra were obtained using a Hitachi F-7000 fluorescence spectrometer equipped with a xenon lamp excitation source. The morphology of the Ag and Ag@PLL-DOX nanoparticles were observed using a TEM (Hitachi H-7650B) at an acceleration voltage of 40 kV, the Ag@PLL-DOX sample was stained with phosphotungstic acid for 15 min before TEM observation. The fluorescence images of the prepared hybrid nanoparticles and the cells were recorded using a confocal laser scanning biological microscope (CLSM; Olympus FV1000-IX81). Cell viability was detected using a Spectra MAX 340 PC plate reader.

Synthesis of Ag Nanoparticles. Ag nanoparticles were synthesized according to the literature.[44] Ten milliliters of freshly prepared 1% $[Ag(NH_3)_2]NO_3$ was added to 10 mL of 2% tannic acid solution at room temperature with vigorous stirring. After 30 min, the resulting Ag colloids were collected and purified three times by centrifugation at 8600 × g for 20 min prior to being redispersed in 20 mL of distilled water.

Synthesis of Amine-Modified Ag Nanoparticles. The prepared Ag nanoparticles were first modified with amino groups. One hundred microliters of Ag nanoparticles was added to 4 mL of a cystamine dihydrochloride solution (0.25 mg/mL) under constant stirring maintaining the reaction for 5 h. Thereafter, the amino-modified Ag nanoparticles were washed and purified three times by centrifugation at 8600 × g for 20 min, and redispersed in 1 mL of distilled water.

Synthesis of Ag@PLL-DOX Nanoparticles. Two hundred microliters of a 5-mM DOX solution was first mixed with 4 mL of a 5-mg/mL PLL solution under gentle stirring. One milliliter of the amino-modified Ag nanoparticle solution was added dropwise into the mixture followed by 500 μL of a DTSSP solution (2.5 mg/mL). The pH value was adjusted between the range of 9−10 with NaOH (1 M) and the mixture stirred at room temperature for 12 h. The obtained Ag@PLL-DOX nanocomposites were separated from the reaction mixture by centrifugation at 8600 × g for 20 min, and redispersed in 100 μL of distilled water. The concentration of DOX was 1 mM, which was calculated by monitoring the absorption of the supernatant liquid.

Drug-Release Assay. A dose of the Ag@PLL-DOX nanoparticle solution was added into 1 mL of an aqueous solution containing varying concentrations of GSH (0−10 mM). The concentration of DOX was maintained at 100 μM. The fluorescence intensity of the mixture was detected after 5 min under excitation at 480 nm.

Cell Culture and Cell Imaging Assay. The human lung carcinoma (A549) cells were grown in a 10% Dulbecco's modified eagle medium, (DMEM), and housed inside a humidified incubator at 37 °C under 5% CO_2 atmosphere. For cell imaging observation, Ag@PLL-DOX nanoparticles were incubated with the A549 cells at a density of 100 000 cells/mL in a 35 mm glass-based dish. The concentration of DOX was 100 μM. After incubation of 1 h, the culture media was removed and the cells were washed with phosphate-buffered saline three times. Each dish was observed by CLSM at 488 nm excitation with the emissions detected in the range of 550−650 nm.

Cell Viability Assay. The cytotoxicity of the nanoparticles were evaluated using the 3-(4,5-dimethylthiazol-2-yl)-2,5-diphenyltetrazolium bromide (MTT) method. A549 cells were seeded in a 96-well culture plate at a density of 1×10^4 cells/well and incubated with Ag@PLL-DOX nanoparticles at 37 °C under 5% CO_2 atmosphere for a determined time. The DOX concentration was maintained at 100 μM. Subsequently, the medium in each well was removed and 100 μL of freshly prepared MTT solution (1 mg/mL) was added to each well and further incubated for 4 h. Next, the supernatant was removed followed by the addition of 100 μL of dimethyl sulfoxide (DMSO). The plate was gently agitated for 5 min and the absorbance of the formed purple formazan at 520 nm was then detected using a Spectra MAX 340PC plate reader.

DOI: 10.1021/acsami.5b03440
ACS Appl. Mater. Interfaces 2015, 7, 13653−13658

RESULTS AND DISCUSSION

Synthesis and Characterization of Ag@PLL-DOX Nanoparticles. The Ag@PLL-DOX nanoparticles were synthesized via a facile one-pot method. Silver nanoparticles were first synthesized through a tannic acid reduction method according to previous literature.[44] To facilitate the subsequent shell coating process, cystamine dihydrochloride was first used to modify the Ag nanoparticles followed by the introduction of amino groups to the surface of the Ag nanoparticles as a result of the strong affinity between Ag and the disulfide groups of cystamine.

The biomolecule, PLL, and anticancer drug, DOX, were assembled onto the Ag nanoparticle surfaces in one step via the water-soluble cross-linker, DTSSP. In this work, the two activated terminal *N*-hydroxysulfosuccinimide esters were the reason DTSSP was chosen as the cross-linker. The *N*-hydroxysulfosuccinimide ester groups can react rapidly and efficiently with the amino groups.[41] Therefore, the DTSSP serves as a cross-linking bridge between the amine-containing PLL molecules and the amine-modified Ag nanoparticle surfaces facilitating the polymer shell formation. At the same time, the amino groups in the DOX molecules can simultaneously cross-link, together with the amino group of the PLL molecules, via the same linkage.[37] Thus, this strategy offers a facile manner to incorporate DOX into the PLL shell during the shell formation process via a one-pot reaction. Additionally, the silver core circumvents the problem of separation, common among organic nanoparticles because of their low nanoparticle weight, and hence the free DOX, yet to be cross-linked, can be efficiently segregated from the as-prepared Ag@PLL-DOX nanoparticles in the reaction mixture via centrifugation. Another advantage of this new adopted method is that as DOX is a fluorescent molecule it offers dual functionality to the Ag@PLL-DOX nanoparticles with both fluorescence and anticancer properties.

The morphology of the Ag and Ag@PLL-DOX nanoparticles were studied by TEM observation. Figure 1a shows the TEM micrograph of the as-prepared Ag nanoparticles. A near spherical morphology is observed with an average diameter of approximately 30 nm. When compared with the TEM micrograph of the Ag@PLL-DOX nanoparticles in Figure 1b, an obvious core−shell hybrid nanoparticle structure can be observed for all the nanoparticles, with an electron dense (dark contrast) Ag core and an electron lean polymer shell (light contrast). The polymer shells are seen to be homogeneous and uniform with an average thickness of ∼7 nm. Thus, the total average diameter of the prepared Ag@PLL-DOX nanoparticles is in the region of 44 nm. The resulting size is beneficial for further drug-delivery applications as small nanoparticles are reported to be easier to accumulate at tumor sites and penetrate deeper into the inner regions of tumor lesions.[42,45]

The UV−vis absorbance spectra of the Ag@PLL-DOX nanoparticles dispersed in aqueous solution is shown in Figure 2a. The surface plasmon absorption of pure Ag nanoparticles and free DOX at the same concentration were also plotted on the same graph for direct comparison. It can be seen that the spectrum of Ag@PLL-DOX hybrid nanoparticles was a superposition of the absorption spectrum of Ag nanoparticles and the free DOX solution. When compared with Ag nanoparticles, a red-shift of the plasmon absorption band of Ag@PLL-DOX can be observed upon the PLL shell coating. The red-shift of the plasmon absorption band of Ag@PLL-DOX can be ascribed to the increase of the refractive index around the Ag nanoparticles after the shell coating. This result correlates with reported observations and also verifies the successful coating of the PLL shell.[22,46] The successful doping of DOX into PLL shell was demonstrated by the CLSM image of Ag@PLL-DOX nanoparticles shown in Figure 2b, from which red fluorescent faculae could be clearly observed relating to DOX. Additionally, the CLSM image also indicates that the nanoparticles are highly dispersed after the drug-doped polymer shell coating.

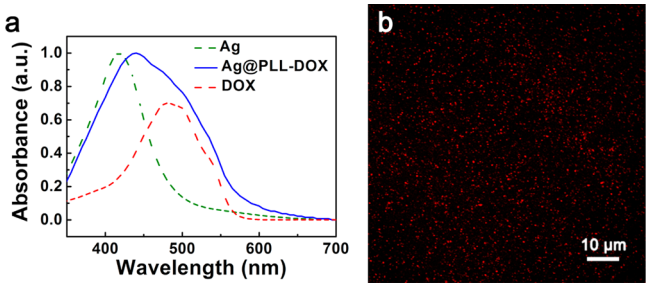

Figure 2. (a) UV−vis absorption spectra of Ag@PLL-DOX nanoparticles (blue line), Ag nanoparticles (green dash), and free DOX (red dash) (b) CLSM image of Ag@PLL-DOX nanoparticles.

To apply the prepared Ag@PLL-DOX nanoparticles in drug delivery, we studied the stability of them at different pH values by fluorescence spectrometer. It was reported that the tumor regions have a slightly acidic pH value as compared with the physiological pH of 7.4. And even healthy cells express a lower pH of 5.5−6.0 in endosomes and approached pH 4.0−5.0 in lysosomes.[47] So we incubated the Ag@PLL-DOX nanoparticles in PBS with different pH values ranging from 3 to 7.4 and studied their fluorescence intensity changes as a function of time. The results showed that all the fluorescence intensity of Ag@PLL-DOX nanoparticles had changed little even after 1 h's incubation, which demonstrated the good pH stability of these nanoparticles in this pH range. It was probably due to the fact that the PLL shell and DOX were cross-linked through covalent bonds by DTSSP that ensures the stability of the shell and minimized the possible leakage of DOX.

Drug-Release Assay. Glutathione is a thiol-containing tripeptide that can be biosynthesized in the body and can reduce disulfide bonds formed in the cytoplasm preventing damage to important cellular components. It has been reported that the extracellular GSH concentration is ∼2 μM, while the intracellular GSH concentration is as high as 10 mM. This dramatic difference in GSH concentration provides an opportunity for designing intracellular-specific drug-delivery systems.[41,48] As the PLL shell and the anticancer drug, DOX, were cross-linked by thiol-cleavable disulfide bonds, it is feasible that the release of the entrapped DOX within the outer shell of the Ag@PLL-DOX nanoparticles can be easily tailored in the presence of GSH as a function of its concentration. Therefore, the Ag@PLL-DOX nanoparticles were incubated in aqueous solutions containing various GSH concentrations, and the emission intensity of each studied by fluorescence spectrometry.

Figure 3 exhibits the relative emission intensity change of the Ag@PLL-DOX nanoparticle solutions as a function of GSH concentration. Fluorescence of the nanoparticles directly related to the DOX doped within the PLL shell under excitation at 480 nm. As can be seen from the spectra, when GSH concentrations are ≤100 μM, the DOX fluorescence

DOI: 10.1021/acsami.5b03440
ACS Appl. Mater. Interfaces 2015, 7, 13653−13658

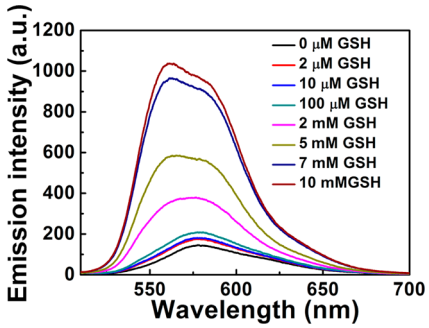

Figure 3. Fluorescence intensity spectra of Ag@PLL-DOX nanoparticle solutions as a function of GSH concentration.

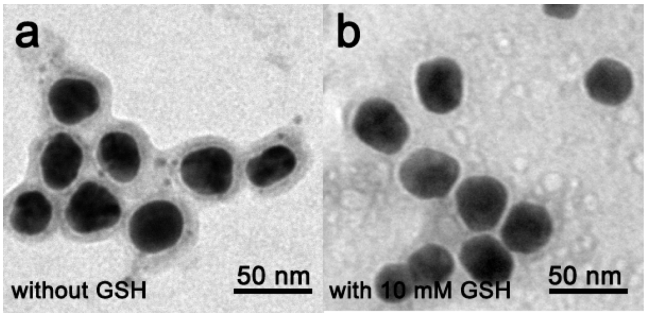

Figure 4. TEM micrographs comparison of Ag@PLL-DOX nanoparticles (a) before and (b) after GSH treatment.

intensity only marginally increases with increasing GSH concentration when compared with a blank, Ag@PLL-DOX in the absence of GSH. However, upon further increases of GSH concentration the fluorescence intensity of DOX increases dramatically, which can be interpreted as fluorescence recovery of DOX and ascribed to two main factors. The first factor relates to the distance-dependent fluorescence quenching effect of the Ag core. Metal nanoparticles are known to greatly quench the fluorescence of fluorophores when in close proximity to their surfaces because of the strong resonant energy transfer from the fluorophore to the metal.[49,50] In the case of the Ag@PLL-DOX nanoparticles, the thin PLL shell retains DOX closely to the Ag nanoparticle surface, thus the resulting DOX fluorescence is greatly quenched by the Ag core because of the near-field interaction. The second factor may lie in localized high concentration of fluorophores that lead to fluorescence self-quenching.[51] Once the entrapped DOX is released, its fluorescence recovery is achieved.

At a low GSH concentration, comparable to the extracellular level (2 μM), minimal disulfide bonds located at the cross-linked sites were cleaved by the thiol-containing GSH. In this case, the PLL shells retain, to a high degree, their cross-linked state and prohibit the majority of DOX from diffusion into the solution. Thus, only slight fluorescence recovery of DOX was observed. However, with increasing GSH concentration, more thiol groups are available to interact with the disulfide bonds and therefore become more susceptible to cleaving, releasing DOX as a consequence resulting in fluorescence recovery, as observed accordingly as the near-field quenching effect of Ag and the self-quenching effect was efficiently avoided.

To further verify the release of DOX, we incubated the Ag@PLL-DOX nanoparticles with a 10-mM GSH solution and thereafter collected by centrifugation and investigated by TEM observation. Figure 4a and 4b provide the TEM micrographs of Ag@PLL-DOX nanoparticles before and after GSH treatment, respectively. In sharp contrast with the core−shell-structured Ag@PLL-DOX nanoparticles (Figure 4a), bare Ag nanoparticles were mainly found after the GSH treatment as shown in Figure 4b. This indicates that a high concentration of GSH facilitates the cleavage of the shell cross-links. The PLL molecules as well as DOX molecules were thus disassembled and dissolved into the solution, yielding bare Ag nanoparticles. Therefore, the fluorescence increase relates to the release of DOX molecules from the shell into the solution. This fluorescence-response behavior provides evidence that GSH facilitated the release of DOX, and the prepared Ag@PLL-DOX nanoparticles minimize the release of entrapped drug molecules before reaching the target tissue—a property of great importance to drug-delivery systems.

Cellular Imaging Assay and Cell Viability Assay. Because the Ag@PLL-DOX nanoparticles show controlled release of DOX upon GSH stimuli, it is critical to determine whether the nanoparticles could internalize into cells, for this drug-release event is only effective within cells. Therefore, a cell imaging assay method was employed to study the cell internalization properties of the Ag@PLL-DOX nanoparticles. A concentrated Ag@PLL-DOX nanoparticle solution was added to 1 mL of an A549 culture medium and the mixture was incubated at 37 °C for 1 h (the final concentration of DOX was 100 μM). After the designated time, the culture media was removed and the cells were washed three times with phosphate-buffered saline buffer. A549 cells cultured without Ag@PLL-DOX nanoparticles were used as a control experiment. Fluorescent confocal microscopy images of the A549 cells are shown in Figure 5, and the fluorescence images were recorded under excitation at 488 nm.

Compared with the image of the cells without addition of nanoparticles (Figure 5a), it is observed that the staining of the cells possessed a high degree of correlation to the Ag@PLL-DOX nanoparticles as bright red fluorescence from the DOX molecules can be clearly seen from Figure 5c, which show the fluorescence image of the cells treated with Ag@PLL-DOX nanoparticles. After overlapping the fluorescence image and the bright-field image of the cells (Figure 5d), it was evidenced that the vast majority of the nanoparticles were observed in the cytoplasm, strongly indicating that the Ag@PLL-DOX nanoparticles were internalized by the cells. Additionally, the Ag@PLL-DOX nanoparticles could be used for efficient cellular imaging.

As the Ag@PLL-DOX nanoparticles were proved to be able to internalize into the cells, we further studied their intracellular drug-release ability via cell viability assay. Ag@PLL-DOX nanoparticles were incubated with A549 cells. Cell viability was studied via the MTT assay as a function of incubation time. The absorbance of MTT at 520 nm is dependent on the degree of cell activation. Cell viability was expressed by the ratio of absorbance of the cells incubated with Ag@PLL-DOX nanoparticles to that of the cells incubated with culture medium only. The data from the plot in Figure 6 show that after incubation for 1.5 h, the cell viability was still as high as 93%, showing good biocompatibility of the Ag@PLL-DOX nanoparticles. This could be because of the fact that during the first 1.5 h, at the intracellular GSH level, only a minority of the disulfide bonds (amine-linkage) were broken by the thiol group of GSH with the PLL shell retaining its cross-linked state that efficiently entrapped the DOX within. Inherently, the

DOI: 10.1021/acsami.5b03440
ACS Appl. Mater. Interfaces 2015, 7, 13653−13658

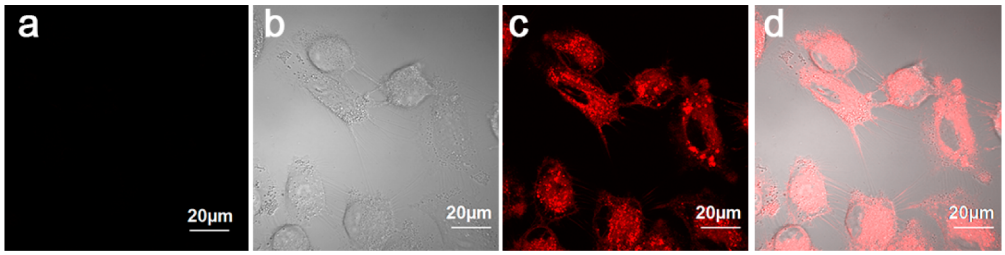

Figure 5. (a) Fluorescence image of A549 cells without treatment of nanoparticles, (b) bright-field image, (c) fluorescence image of A549 cells incubated with Ag@PLL-DOX nanoparticles for 1 h at 37 °C, (d) the overlapped image of (b) and (c).

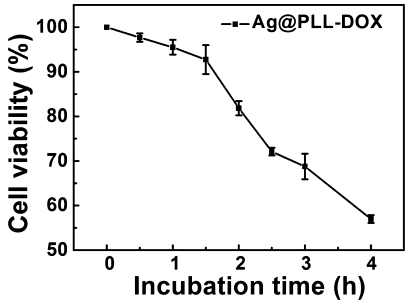

Figure 6. Cell viability ratio of cells incubated with Ag@PLL-DOX nanoparticles as a function of incubation time.

biocompatible PLL shell allows the Ag@PLL-DOX nanoparticles to have low cytotoxicity.

With increasing incubating time, further cross-linked sites were cleaved by GSH resulting in the PLL shell gradually disassembling in the cells leading to the large release of trapped DOX. Thus, a dramatic decrease of the cell viability was observed. Furthermore, the viability ratio reduced to ∼55% after a short incubation time of 4 h. The results demonstrate the controlled nature of the drug-release properties of the prepared Ag@PLL-DOX nanoparticles, which is significant for its use as an efficient drug-delivery system.

CONCLUSION

Core−shell fluorescent nanoparticles of Ag@PLL-DOX were prepared. The biomolecule PLL, and fluorescent anticancer drug DOX, were successfully assembled onto the Ag nanoparticle surfaces by a facile one-pot method via the disulfide cross-linker DTSSP. As the disulfide bond of DTSSP can be cleaved by the thiol group, GSH-mediated drug-release behavior of the Ag@PLL-DOX nanoparticles was observed. The release of DOX upon different GSH concentrations was detected via the fluorescence-recovering phenomenon of DOX related to the distance-dependent fluorescence quenching effect of the silver core. Fluorescence images of the cells proved the cell internalization ability of the prepared Ag@PLL-DOX nanoparticles. Cellular viability assaying demonstrated that the Ag@PLL-DOX nanoparticles possess good biocompatibility and terminate cells efficiently upon DOX release at the intracellular GSH concentration. Tailoring such properties provide promising applications of the Ag@PLL-DOX nanoparticles as a specific drug-delivery system.

AUTHOR INFORMATION

Corresponding Authors

*E-mail: lidong@mater.ustb.edu.cn.
*E-mail: tangfu@ustb.edu.cn.

Notes

The authors declare no competing financial interest.

ACKNOWLEDGMENTS

This work was supported by the National Natural Science Foundation of China (51403018, 51373022), the Fundamental Research Funds for the Central Universities (FRF-TP-14-002A1). The authors thank Dr. Libin Liu for giving support for the cellular experiments.

REFERENCES

(1) Xu, X.; Chen, S.; Li, L.; Yu, G.; Di, C.; Liu, Y. Photophysical Properties of Polyphenylphenyl Compounds in Aqueous Solutions and Application of Their Nanoparticles for Nucleobase Sensing. *J. Mater. Chem.* **2008**, *18*, 2555−2561.

(2) Wang, X.; He, F.; Li, L.; Wang, H.; Yan, R.; Li, L. Conjugated Oligomer-Based Fluorescent Nanoparticles as Functional Nanocarriers for Nucleic Acids Delivery. *ACS Appl. Mater. Interfaces* **2013**, *5*, 5700−5708.

(3) Feng, L.; Zhu, C.; Yuan, H.; Liu, L.; Lv, F.; Wang, S. Conjugated Polymer Nanoparticles: Preparation, Properties, Functionalization and Biological Applications. *Chem. Soc. Rev.* **2013**, *42*, 6620−6633.

(4) Feng, L.; Liu, L.; Lv, F.; Bazan, G. C.; Wang, S. Preparation and Biofunctionalization of Multicolor Conjugated Polymer Nanoparticles for Imaging and Detection of Tumor Cells. *Adv. Mater.* **2014**, *26*, 3926−3930.

(5) Chong, H.; Zhu, C.; Song, J.; Feng, L.; Yang, Q.; Liu, L.; Lv, F.; Wang, S. Preparation and Optical Property of New Fluorescent Nanoparticles. *Macromol. Rapid Commun.* **2013**, *34*, 736−742.

(6) Feng, X.; Lv, F.; Liu, L.; Tang, H.; Xing, C.; Yang, Q.; Wang, S. Conjugated Polymer Nanoparticles for Drug Delivery and Imaging. *ACS Appl. Mater. Interfaces* **2010**, *2*, 2429−2435.

(7) Feng, X.; Tang, Y.; Duan, X.; Liu, L.; Wang, S. Lipid-Modified Conjugated Polymer Nanoparticles for Cell Imaging and Transfection. *J. Mater. Chem.* **2010**, *20*, 1312−1316.

(8) He, Y.; Kang, Z.-H.; Li, Q.-S.; Tsang, C. H. A.; Fan, C.-H.; Lee, S.-T. Ultrastable, Highly Fluorescent, and Water-Dispersed Silicon-Based Nanospheres as Cellular Probes. *Angew. Chem., Int. Ed.* **2009**, *48*, 128−132.

(9) Pei, H.; Li, F.; Wan, Y.; Wei, M.; Liu, H.; Su, Y.; Chen, N.; Huang, Q.; Fan, C. Designed Diblock Oligonucleotide for the Synthesis of Spatially Isolated and Highly Hybridizable Functionalization of DNA-Gold Nanoparticle Nanoconjugates. *J. Am. Chem. Soc.* **2012**, *134*, 11876−11879.

(10) Caruso, F. Nanoengineering of Particle Surfaces. *Adv. Mater.* **2001**, *13*, 11−22.

(11) Yan, Y.; Björnmalm, M.; Caruso, F. Assembly of Layer-by-Layer Particles and Their Interactions with Biological Systems. *Chem. Mater.* **2014**, *26*, 452−460.

(12) Luo, Z.; Yuan, X.; Yu, Y.; Zhang, Q.; Leong, D. T.; Lee, J. Y. From Aggregation-Induced Emission of Au (I)-Thiolate Complexes to Ultrabright Au(0)@Au(I)-Thiolate Core-Shell Nanoclusters. *J. Am. Chem. Soc.* **2012**, *134*, 16662−16670.

DOI: 10.1021/acsami.5b03440
ACS Appl. Mater. Interfaces 2015, 7, 13653−13658

(13) Cassette, E.; Pons, T.; Bouet, C.; Helle, M.; Bezdetnaya, L.; Marchal, F.; Dubertret, B. Synthesis and Characterization of Near-Infrared Cu-In-Se/ZnS Core/Shell Quantum Dots for In vivo Imaging. *Chem. Mater.* **2010**, *22*, 6117−6124.
(14) Lv, W.; Feng, J.; Yan, W.; Faul, C. F. J. Self-Assembly and pH Response of Electroactive Liquid Core-Tetra(aniline) Shell Microcapsules. *J. Mater. Chem. B* **2014**, *2*, 4720−4725.
(15) Kim, K.; Webster, S.; Levi, N.; Carroll, D. L.; Pinto, M. R.; Schanze, K. S. Luminescent Core-Shell Photonic Crystals from Poly(phenylene ethynylene) Coated Silica Spheres. *Langmuir* **2005**, *21*, 5207−5211.
(16) Radmilovic, V.; Ophus, C.; Marquis, E. A.; Rossell, M. D.; Tolley, A.; Gautam, A.; Asta, M.; Dahmen, U. Highly Monodisperse Core-Shell Particles Created by Solid-State Reactions. *Nat. Mater.* **2011**, *10*, 710−715.
(17) Cui, Q.; He, F.; Wang, X.; Xia, B.; Li, L. Gold Nanoflower@Gelatin Core-shell Nanoparticles Loaded with Conjugated Polymer Applied for Cellular Imaging. *ACS Appl. Mater. Interfaces* **2013**, *5*, 213−219.
(18) Xia, B.; Wang, X.; He, F.; Cui, Q.; Li, L. Self-Assembly of Conjugated Polymer on Hybrid Nanospheres for Cellular Imaging Applications. *ACS Appl. Mater. Interfaces* **2012**, *4*, 6332−6337.
(19) Pastoriza-Santos, I.; Pérez-Juste, J.; Liz-Marzán, L. M. Silica-Coating and Hydrophobation of CTAB-Stabilized Gold Nanorods. *Chem. Mater.* **2006**, *18*, 2465−2467.
(20) Cheng, D.; Xu, Q.-H. Separation Distance Dependent Fluorescence Enhancement of Fluorescein Isothiocyanate by Silver Nanoparticles. *Chem. Commun.* **2007**, 248−250.
(21) Zhao, T.; Wu, H.; Yao, S. Q.; Xu, Q.-H.; Xu, G. Q. Nanocomposites Containing Gold Nanorods and Porphyrin-Doped Mesoporous Silica with Dual Capability of Two-Photon Imaging and Photosensitization. *Langmuir* **2010**, *26*, 14937−14942.
(22) Tang, F.; He, F.; Cheng, H.; Li, L. Self-Assembly of Conjugated Polymer-Ag@SiO_2 Hybrid Fluorescent Nanoparticles for Application to Cellular Imaging. *Langmuir* **2010**, *26*, 11774−11778.
(23) Skirtach, A. G.; Yashchenok, A. M.; Möhwald, H. Encapsulation, Release and Applications of LbL Polyelectrolyte Multilayer Capsules. *Chem. Commun.* **2011**, *47*, 12736−12746.
(24) Caruso, F.; Donath, E.; Möhwald, H. Influence of Polyelectrolyte Multilayer Coatings on Förster Resonance Energy Transfer between 6-Carboxyfluorescein and Rhodamine B-Labeled Particles in Aqueous Solution. *J. Phys. Chem. B* **1998**, *102*, 2011−2016.
(25) Klitzing, R. V.; Möhwald, H. A Realistic Diffusion Model for Ultrathin Polyelectrolyte Films. *Macromolecules* **1996**, *29*, 6901−6906.
(26) Donath, E.; Sukhorukov, G. B.; Caruso, F.; Davis, S. A.; Möhwald, H. Novel Hollow Polymer Shells by Colloid-Templated Assembly of Polyelectrolytes. *Angew. Chem., Int. Ed.* **1998**, *37*, 2202−2205.
(27) Sukhorukov, G. B.; Antipov, A. A.; Voigt, A.; Donath, E.; Möhwald, H. pH-Controlled Macromolecule Encapsulation in and Release from Polyelectrolyte Multilayer Nanocapsules. *Macromol. Rapid Commun.* **2001**, *22*, 44−46.
(28) Zheludkevich, M. L.; Shchukin, D. G.; Yasakau, K. A.; Möhwald, H.; Ferreira, M. G. S. Anticorrosion Coating with Self-Healing Effect Based on Nanocontainers Impregnated with Corrosion Inhibitor. *Chem. Mater.* **2007**, *19*, 402−411.
(29) Tang, F.; Wang, X.; Xu, X.; Li, L. Phytic Acid Doped Nanoparticles for Green Anticorrosion Coatings. *Colloids Surf., A* **2010**, *369*, 101−105.
(30) Wang, X.; He, F.; Tang, F.; Ma, N.; Li, L. Preparation of Hybrid Fluorescent-Magnetic Nanoparticles for Application to Cellular Imaging by Self-Assembly. *Colloids Surf., A* **2011**, *392*, 103−109.
(31) Tang, F.; Ma, N.; Wang, X.; He, F.; Li, L. Hybrid Conjugated Polymer-Ag@PNIPAM Fluorescent Nanoparticles with Metal-Enhanced Fluorescence. *J. Mater. Chem.* **2011**, *21*, 16943−16948.
(32) Huang, Y.; Lin, W.; Chen, K.; Zhang, W.; Chen, X.; Zhang, M. Q. Thermoresponsive Fluorescence of A Graphene-Polymer Composite Based on A Local Surface Plasmon Resonance Effect. *Phys. Chem. Chem. Phys.* **2014**, *16*, 11584−11589.
(33) Chakraborty, P.; Bairi, P.; Roy, B.; Nandi, A. K. Rheological and Fluorescent Properties of Riboflavin-Poly(*N*-isopropylacrylamide) Hybrid Hydrogel with A Potentiality of Forming Ag Nanoparticle. *RSC Adv.* **2014**, *4*, 54684−54693.
(34) Corbitt, T. S.; Sommer, J. R.; Chemburu, S.; Ogawa, K.; Ista, L. K.; Lopez, G. P.; Whitten, D. G.; Schanze, K. S. Conjugated Polyelectrolyte Capsules: Light-Activated Antimicrobial Micro "Roach Motels. *ACS Appl. Mater. Interfaces* **2009**, *1*, 48−52.
(35) Roy, D.; Cambra, J. N.; Sumerlin, B. S. Future Perspectives and Recent Advances in Stimuli-Responsive Materials. *Prog. Polym. Sci.* **2010**, *35*, 278−301.
(36) Zhang, J.; Ma, N.; Tang, F.; Cui, Q.; He, F.; Li, L. pH- and Glucose-Responsive Core-shell Hybrid Nanoparticles with Controllable Metal-Enhanced Fluorescence Effects. *ACS Appl. Mater. Interfaces* **2012**, *4*, 1747−1751.
(37) Santra, S.; Kaittanis, C.; Santiesteban, O. J.; Perez, J. M. Cell-Specific, Activatable, and Theranostic Prodrug for Dual-Targeted Cancer Imaging and Therapy. *J. Am. Chem. Soc.* **2011**, *133*, 16680−16688.
(38) Miyata, T.; Asami, N.; Uragami, T. Preparation of an Antigen-Sensitive Hydrogel Using Antigen-Antibody Bindings. *Macromolecules* **1999**, *32*, 2082−2084.
(39) Li, G. L.; Möhwald, H.; Shchukin, D. G. Precipitation Polymerization for Fabrication of Complex Core-Shell Hybrid Particles and Hollow Structures. *Chem. Soc. Rev.* **2013**, *42*, 3628−3646.
(40) Shutava, T. G.; Pattekari, P. P.; Arapov, K. A.; Torchilin, V. P.; Lvov, Y. M. Architectural Layer-by-Layer Assembly of Drug Nanocapsules with PEGylated Polyelectrolytes. *Soft Matter* **2012**, *8*, 9418−9427.
(41) Koo, A. N.; Lee, H. J.; Kim, S. E.; Chang, J. H.; Park, C.; Kim, C.; Park, J. H.; Lee, S. C. Disulfide-Cross-Linked PEG-Poly(amino acid)s Copolymer Micelles for Glutathione-Mediated Intracellular Drug Delivery. *Chem. Commun.* **2008**, 6570−6572.
(42) Wei, T.; Chen, C.; Liu, J.; Liu, C.; Posocco, P.; Liu, X.; Cheng, Q.; Huo, S.; Liang, Z.; Fermeglia, M.; Pricl, S.; Liang, X.-J.; Rocchi, P.; Peng, L. Anticancer Drug Nanomicelles Formed by Self-Assembling Amphiphilic Dendrimer to Combat Cancer Drug Resistance. *Proc. Natl. Acad. Sci. U.S.A.* **2015**, *112*, 2978−2983.
(43) Kim, J.; Lee, Y. M.; Kang, Y.; Kim, W. J. Tumor-Homing, Size-Tunable Clustered Nanoparticles for Anticancer Therapeutics. *ACS Nano* **2014**, *8*, 9358−9367.
(44) Sivaraman, S. K.; Elango, I.; Kumar, S.; Santhanam, V. A Green Protocol for Room Temperature Synthesis of Silver Nanoparticles in Seconds. *Curr. Sci.* **2009**, *97*, 1055−1059.
(45) Cabral, H.; Matsumoto, Y.; Mizuno, K.; Chen, Q.; Murakami, M.; Kimura, M.; Terada, Y.; Kano, M. R.; Miyazono, K.; Uesaka, M.; Nishiyama, N.; Kataoka, K. Accumulation of Sub-100 nm Polymeric Micelles in Poorly Permeable Tumours Depends on Size. *Nat. Nanotechnol.* **2011**, *6*, 815−823.
(46) Chen, H.; Ming, T.; Zhao, L.; Wang, F.; Sun, L.-D.; Wang, J.; Yan, C.-H. Plasmon-Molecule Interactions. *Nano Today* **2010**, *5*, 494−505.
(47) Stenzel, M. H. RAFT Polymerization: An Avenue to Functional Polymeric Micelles for Drug Delivery. *Chem. Commun.* **2008**, 3486−3503.
(48) Jones, D. P.; Carlson, J. L.; Samiec, P. S.; Sternberg, P.; Mody, V. C.; Reed, R. L.; Brown, L. A. S. Glutathione Measurement in Human Plasma Evaluation of Sample Collection, Storage and Derivatization Conditions for Analysis of Dansyl Derivatives by HPLC. *Clin. Chim. Acta* **1998**, *275*, 175−184.
(49) Lakowicz, J. R. Radiative Decay Engineering: Biophysical and Biomedical Applications. *Anal. Biochem.* **2001**, *298*, 1−24.
(50) Aslan, K.; Pérez-Luna, V. H. Quenched Emission of Fluorescence by Ligand Functionalized Gold Nanoparticles. *J. Fluoresc.* **2004**, *14*, 401−405.
(51) Li, K.; Liu, B. Polymer-Encapsulated Organic Nanoparticles for Fluorescence and Photoacoustic Imaging. *Chem. Soc. Rev.* **2014**, *43*, 6570−6597.

DOI: 10.1021/acsami.5b03440
ACS Appl. Mater. Interfaces 2015, 7, 13653−13658